

Optimization of synthesis and basic characterization of 55PbO-10ZnO-35P₂O₅ glass modified by CoO

Jan Smolík^{1*}, Petr Knotek¹, Jiří Schwarz¹, Petr Kutálek²,
Miloslav Pouzar³, and Eva Černošková²

¹ *Department of General and Inorganic Chemistry, University of Pardubice,
CZ–532 10 Pardubice, Czech Republic*

² *Joint Laboratory of Solid State Chemistry, University of Pardubice,
CZ–532 10 Pardubice, Czech Republic*

³ *Institute of Environmental and Chemical Engineering, University of Pardubice,
CZ–532 10 Pardubice, Czech Republic*

Received: May 28, 2020; Accepted: June 10, 2020

This work is focused on the optimization of preparation of Pb-rich 55PbO-10ZnO-35P₂O₅ phosphate glass modified by cobalt(II) dioxide, CoO, exhibiting the absorption bands in the visible region. The most suitable glasses were obtained using so-called wet method, which means using dilute H₃PO₄ and Co(NO₃)₂·6H₂O. The prepared glasses were optically transparent, homogeneous in the whole volume, without bubbles, defects, cracks or crystals. Consequently, the glasses have been characterized using different methods in order to determine properties, such as the density, molar volume, structure, thermal properties (glass transition temperature and coefficient of thermal expansion), optical properties (colour change and absorption in the visible region), or electrical properties (DC conductivity). The influence of the content of CoO (0–3.55 mol. %) on the selected properties is discussed in detail. In practical applications, CoO-modified glasses are used especially in blue coloured glasses or as optical filters, acid-base or radiation-sensitive indicators, and as possible candidate for tunable solid-state lasers matrix and the materials suitable for direct laser writing at a wavelength of 532 nm.

Keywords: Phosphate glasses; Preparation; Properties; Cobalt (II) oxide

* Corresponding author, ✉ jan.smolik@student.upce.cz

Introduction

Phosphate glasses are a special group of oxide glasses containing P_2O_5 as a network former [1,2]. In comparison with the conventional oxide glasses (silicate, borosilicate, etc.), this type of material possesses lower synthesis and glass transition temperatures, a higher value of the thermal expansion coefficient and high solubility for rare-earth ions [3]. The main problem of some phosphate glasses is their low chemical stability and durability at the ambient atmosphere and in water media [3,4]. The durability can be improved by the addition of the modifying oxides, frequently, the transition metal oxides (e.g. iron oxide [5]). Nevertheless, due to the above-mentioned reasons, phosphate glasses are promising materials for many technological applications such as biomedical use [6]. These materials can also be used for the metal sealing [7], for the storage of nuclear waste [5] or as devices in optics (solid state lasers [8], low-frequency optical fibers [9], or optical memory [10], etc.).

Phosphate glasses are usually transparent in the whole visible region with the short wavelength absorption edge in the UV region [11,12]. Various modifying oxides, especially transition metal oxides (CoO, NiO), can be used for the change of colour manifested itself by the presence of absorption bands. The decrease of transmission caused by the transition-metal oxides is promising for some optical applications; for instance, as UV-transmitting optical filters with low transmission in the visible region [13].

Cobalt can be present in glasses in three various forms. Metallic cobalt particles are formed using the reduction conditions during the synthesis and cause red-brown colour of the glass. Co in glasses can occur also as the ions, either as trivalent Co^{3+} or bivalent Co^{2+} . During the strong oxidative melting conditions, the ratio of Co^{3+} strongly increases, especially in alkali-rich glasses, and the colour of prepared glasses is green-yellow. However, in most cases, including our phosphate glasses, glasses contain the Co^{2+} ions that can exist in two different coordinations: tetrahedral (predominant form) and octahedral. The coordination of Co^{2+} ions determines the final colour of the glass – blue (tetrahedral) and pink (octahedral). In addition, the intensity of the resultant colour depends on the glassy matrix as well, e.g., the extinction coefficient of Co^{2+} ions in phosphate glasses is lower in comparison with those in silicates due to the different coupling modes [2,13].

The main aim of this work is to optimize the preparation and basic characterization of Pb-rich phosphate glasses $55PbO-10ZnO-35P_2O_5$ modified by the various amounts of CoO (0–3.55 mol. %, calculated as the molar content of CoO and with respect to the total moles of all the constituents contained in the glass.). The above-mentioned composition was chosen because of the presence of zinc oxide that causes the increase of chemical durability (comparable to the classic “windows glasses”) and the high amount of lead oxide (55 mol. %) increases the refractive index and its non-linearity [14–16].

These properties are important for practical applications (e.g. as a part of passive optical elements). The incorporation of CoO into the glassy matrix induces the absorption in the visible region including a wavelength of 532 nm that is important for a direct-laser-writing capability because the most intensive and cheapest lasers in the industry emit just at this wavelength. Consequently, the prepared homogenous glassy materials containing CoO could be used for direct laser writing into the microlenses.

Materials and methods

Preparation of glassy materials was optimized. The optimization is described in detail below. For the preparation of glasses the following substances were used: ZnO, PbO (both Aldrich, St. Louis, MO, USA), two different P sources: H_3PO_4 (99.9% purity, Penta, Chrudim, Czech Republic) and $\text{NH}_4\text{H}_2\text{PO}_4$ (Acros Organics, Fisher Scientific, Pardubice, Czech Republic) plus three different Co sources: Co, Co_3O_4 , and $\text{Co}(\text{NO}_3)_2 \cdot 6\text{H}_2\text{O}$ (all from Lachema, Brno, Czech Republic). The selected combination of starting materials was weighted (20 g batches) into a corundum crucible and the mixture thoroughly homogenized (and dried in the case of H_3PO_4).

The corundum crucible was inserted into a muffle furnace. Subsequently, the decomposition (in the case of $\text{NH}_4\text{H}_2\text{PO}_4$ and/or $\text{Co}(\text{NO}_3)_2 \cdot 6\text{H}_2\text{O}$) was done at 200 °C for 60 min and the mixture obtained was heated up to the synthesis temperature (1050 °C). Finally, the melt was poured onto a nickel plate and the final glassy material obtained during the cooling down on the air.

The content of Co in the prepared glasses was verified by XRF analysis (desktop energy dispersive ElvaX, Elvatech, Kiev, Ukraine; equipped with the Pd anode). The density was determined by the Archimedean method using distilled water as a liquid medium. Molar volume was calculated from the obtained density (see below). The thermal properties (bulk sample ($10 \times 5 \times 5 \text{ mm}^3$)) were examined by the means of the Thermomechanical Analysis (TMA CX04R, RMI; Lázně Bohdaneč, Czech Republic) and Differential Thermal Analysis (DTA 03, RMI) employing powdered samples for the latter. In both cases, the heating rate of 5 °C min^{-1} was used. The optical transmission was measured in the spectral region of 200–800 nm using a UV/Vis Spectrometer Lambda 12 (Perkin-Elmer, Waltham, MA, USA). For this measurement, the samples were polished to the optical quality using the alumina (50 nm particle size) suspension in glycerol on the Minimet 1000 instrument (Buehler, Lake Bluff, IL, USA). Information on the structure was examined by Raman microscope (Dimension P2, Lambda Solution; Vancouver, Canada) operating at 785 nm. The reduced Raman spectra were calculated according to Shukker-Gammon equation [17]. The DC electrical conductivity via the V-A characteristic (from -3 to $+3$ V) was measured with a picoammeter (Keithley 648; Tektronix, Beaverton, OR, USA) at temperatures 30–300 °C at heating rate of 2 °C min^{-1} was performed.

Results and discussion

Synthesis optimization

As the glasses selected will be used in the subsequent studies on direct laser writing, they should be well transparent, homogeneous in the whole volume, without bubbles, defects, cracks, and crystalline particles. Consequently, the influence of (i) Co sources and (ii) P₂O₅ sources on the above-mentioned properties was examined.

(i) Three different Co sources were used: (a) The powder metallic Co can lead to the formation of defect states in the glassy structure, but it does not contain undesirable impurities; (b) Co₃O₄ is the most thermodynamically stable compound suitable for our glasses modification, and (c) Co(NO₃)₂·6H₂O which due to the decomposition into NO_x and H₂O enhances the melt homogeneity and ensures a better homogeneity of the final glass formed.

In the case of using metallic Co powder, not required blue but grey glass was formed; the final colour depending on the Co powder concentration. The powdered metallic Co was not probably completely dissolved and thus Co was only partially oxidized during the melting process, which gave rise to a dispersion in the glassy matrix with the formation of a grey colour tone. The similar effect could be observed during a glass preparation in platinum crucible, where the platinum can be incorporated into the glass matrix followed by the colour change.

Subsequently, both Co₃O₄ and Co(NO₃)₂·6H₂O were tested as the sources of Co ions. Both materials provided CoO resulting in the blue colour of glass since Co³⁺ ions in Co₃O₄ were reduced to Co²⁺ during the synthesis at a temperature of about 900 °C [18]. Nevertheless, for further experiments, we selected the nitrate because the glasses with a better homogeneity in overall.

(ii) Two different sources of P₂O₅ were examined having resulted in two completely different ways of glassy precursor preparation. *The dry method* utilised NH₄H₂PO₄, whereas *the wet method* was based on the use of dilute H₃PO₄. The former method had led to the formation of glass that contained large amounts of bubbles that could not be removed by further remelting because of unwanted crystallization. The use of H₃PO₄ water solution had then resulted in a homogenous suspension of glassy precursor and the glass obtained was homogeneous and without bubbles. From these reasons, the *wet method* was selected for further experiments. A set of samples of glassy 55PbO-10ZnO-35P₂O₅ modified by various concentrations of CoO (0–3.55 mol. %) was prepared by the *wet method* using Co(NO₃)₂·6H₂O as the source of Co²⁺ ions at the temperature of *ca.* 1050 °C. The glasses prepared by this method were transparent, homogeneous in the whole volume, without bubbles, defects, cracks, and crystalline particles. The real Co content in the prepared glasses was verified by means of the XRF analysis.

The unmodified 55PbO-10ZnO-35P₂O₅ glass was colorless while the presence of 0.15 mol. % of CoO in the glassy matrix had caused a blue colouring of the glass with no evident crystallization. As the content of CoO had increased, the blue colour of the glass became more intensive. Glass with the highest CoO content (3.55 mol. %) seemed to be almost black. Such a result was in good agreement with the literature [2].

Density, molar volume

The prepared phosphate glasses were analysed using several methods to obtain the basic characteristics. Density was determined employing the Archimedes' method. In the case of measurements, the density of solid state (ρ_s) on the air was calculated according to the equation [19]:

$$\rho_s = \frac{\rho_l \cdot m_1}{m_1 - \rho_l} \quad (1)$$

where ρ_l is the density of used liquid media (distilled water in our case) and m_1 and m_2 are the sample weight on the air and in a liquid media, respectively. Furthermore, the experimental data were compared to the calculated ones. Since the density is not an additive quantity, the calculated values have to be determined as a ratio of the molar mass and calculated molar volume.

Molar volume of a multicomponent glass (V_M) is an additive measure and, in the first approximation, can be estimated using the simplest mixing rule which is valid for the systems with ideal behaviour (the individual components being immiscible and without any interaction with each other):

$$V_{M, \text{calc.}} = \sum_j x_j V_{j, \text{calc.}} \quad (2)$$

where x_j is the molar fraction of each oxide in the system and $V_{j, \text{calc.}}$ is the value of molar volume corresponding to the corresponding oxide ($V_m(\text{PbO}) = 23.42 \text{ cm}^3 \text{ mol}^{-1}$, $V_m(\text{ZnO}) = 14.50 \text{ cm}^3 \text{ mol}^{-1}$, $V_m(\text{P}_2\text{O}_5) = 59.39 \text{ cm}^3 \text{ mol}^{-1}$, $V_m(\text{CoO}) = 11.64 \text{ cm}^3 \text{ mol}^{-1}$). Subsequently, the experimental molar volume was determined as the ratio of molar mass of synthesized material and the required density measured.

In Fig. 1a, one can see that the experimental and calculated values of density have exhibited almost the same trend. The experimental values were higher compared to the calculated ones, because the conditions of the mixing model were violated (see Experimental) and the high concentration of PbO allowed smaller ions ($r(\text{P}^{5+}) = 0.29 \text{ \AA}$, $r(\text{Zn}^{2+}) = 0.75 \text{ \AA}$, $r(\text{Co}^{2+}) = 0.7 \text{ \AA}$) to be incorporated into vacancies formed by larger Pb^{2+} ions ($r(\text{Pb}^{2+}) = 1.18 \text{ \AA}$).

The obtained density slightly increased from 5.54 to 5.63 g cm⁻³ with the CoO content increasing from 0 to 3.55 mol. %. The reason for the observed increase of density is probably a high value of CoO density (6.44 g cm⁻³) [20].

Fig. 1b shows the role of the CoO content on the molar volume. The experimental molar volume decreased from 32.6 to 31.0 cm³ mol⁻¹ with the increasing CoO content. In this case, the decrease was apparently caused by the significantly lower value of the molar volume for CoO in comparison with the other oxides present (i.e., ZnO, PbO, and P₂O₅). Experimental and calculated values of the molar volume showed the same trend.

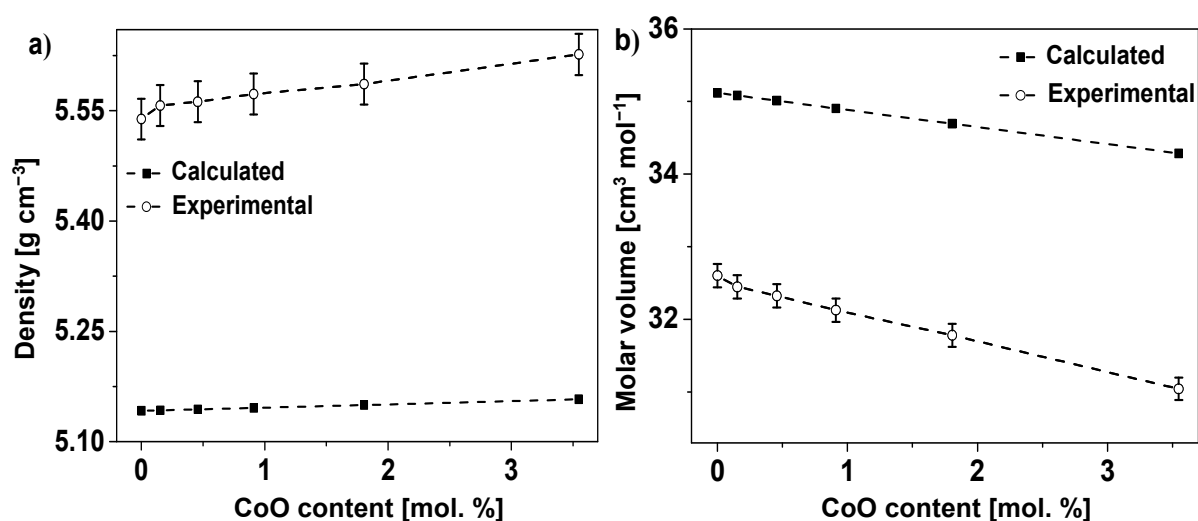


Fig. 1 The dependency of experimental density (a) and molar volume (b) on the CoO content for the prepared glasses and their comparison with the calculated ones (dashed lines with full black cubes)

Thermal properties

These include the glass transition temperature (T_g) and the coefficient of thermal expansion (CTE), both investigated using the Thermomechanical Analysis (TMA); Fig. 2. The value of T_g was determined as the intersection of tangents for glass and undercooled liquid region. CTE was then evaluated as the slope of linear dependence of thermal expansion in the temperature range of 100–300 °C. In addition, T_g was determined by means of Differential Thermal Analysis (DTA; see again Fig. 2). In this case, T_g was evaluated as the mid-point in the glass transition region. Both T_g values obtained using the different types of samples (powder vs. bulk) and the two methods (DTA vs. TMA) are in a good agreement.

In Table 1, the values of T_g and CTE determined by TMA for the glasses with the various content of CoO are summarized. The T_g value rapidly increased after the first addition of CoO from 359 to 377 °C for unmodified and glass containing 0.15 mol. % of CoO, respectively. Then T_g decreased to 367 °C (0.46 mol. % CoO) and subsequently T_g value slightly increased with the increasing CoO content. CTE reached the values in the range of 14.62–15.20 ppm K⁻¹ for 0.15–3.55 mol. % of CoO. Comparing to the T_g dependence, the first addition of 0.15 mol. % of CoO into the glassy matrix caused a big drop of CTE by ≈ 2 ppm K⁻¹. The next increase of CoO content did not affect this value significantly. It should be noted that the increase of the glass transition temperature and decrease of the coefficient of thermal expansion are interrelated and usually being attributed to the structure strengthening [21].

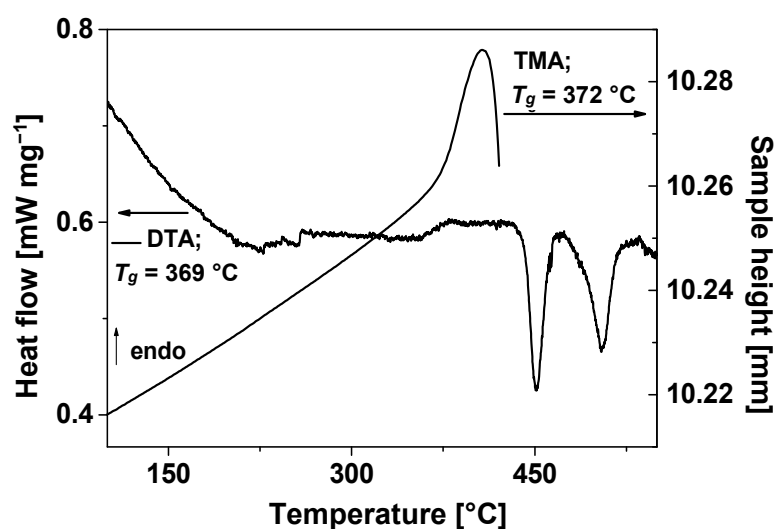


Fig. 2 Determination of thermal properties by the various ways

T_g by DTA (powder form); T_g and CTE by TMA (bulk sample); both for 0.91 mol. % of CoO

Table 1 The values of T_g and CTE (determined in the range 100–300 °C) for the glasses containing various content of CoO (0–3.55 mol. %) obtained by TMA

CoO content [mol. %]	T_g [°C]	CTE (100–300 °C) [ppm K ⁻¹]
0	359	16.72
0.15	377	14.62
0.46	367	14.93
0.91	371	15.20
1.81	374	14.69
3.55	383	14.80

Optical transmission

The optical transmission was measured on the polished samples using UV/Vis spectrometer. The unmodified glassy 55PbO-10ZnO-35P₂O₅ matrix was transparent in the whole visible region and its short wavelength absorption edge was located in the UV region (UV cut-off \approx 290 nm); see Fig. 3a. The CoO addition did not significantly affect the position of this UV-cut off. However, it led to the rise of the absorption band in the range \approx 400–700 nm formed by at least three different bands (\approx 532 nm; \approx 579 nm and \approx 625 nm). The intensity of this absorption band increased almost linearly with the increasing CoO content.

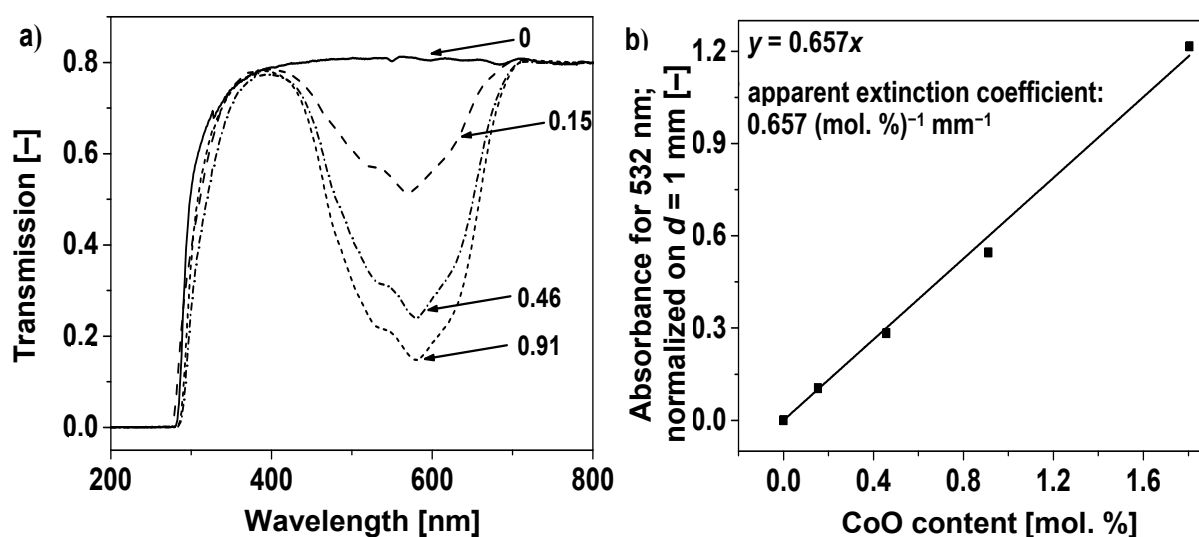


Fig. 3 Spectral dependence of optical transmission for selected samples (the values refer to the CoO content in mol. %) (a) and determination of the apparent extinction coefficient according to the Lambert–Beer law (b)

The origin of the relative broad band is connected with the presence of Co²⁺ ion in d⁷ electron configuration. Based on the ligand-field theory [22], the signal might be splitted by distortion of the d-orbitals of Co²⁺ ion. Consequently, the permitted d-d transitions between different energy levels determine the number of absorption bands present in the spectrum. As the oxygen causes a low splitting of d-orbitals, high-spin tetrahedral (T_d) and/or octahedral (O_h) complexes can be formed. The simplified case of the d-orbitals splitting is shown in Fig. 4, assuming that, during the illumination, d-electrons move to the higher energy levels; e.g., t₂ in the tetrahedral coordination. We suppose that this may explain why we have observed several absorption bands in the visible region. Finally, an absorption at 532 nm can be assigned to the d-d transition in octahedrally coordinated Co²⁺ ions [23].

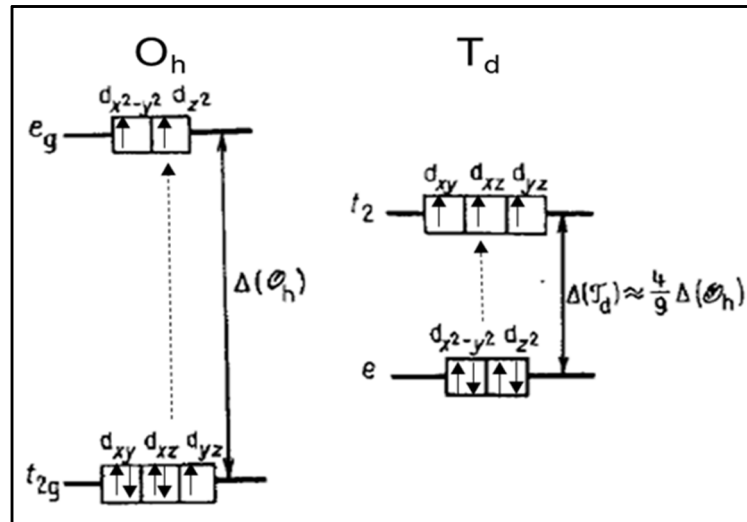


Fig. 4 Schematic illustration of d-orbitals splitting in octahedrally (O_h) or tetrahedrally (T_d) coordinated Co^{2+} caused by the oxygen atoms, dashed lines illustrate possible d-d transitions [22]

We shall characterize the Co^{2+} ions by the absorption band at a wavelength of 532 nm, which is a value widely used for the lasers in many technical applications. In Fig. 3b, it is seen that the absorption, normalized with respect to the sample thickness (1 mm), has exhibited the linear dependence on the CoO content. Thus, the optical behaviour of the samples at this wavelength fulfilled the Lambert–Beer law. The slope of this dependence was calculated for the content of CoO between 0 to 1.81 mol. % because the Lambert–Beer law was not applicable to a higher content due to the too high absorption. The respective slope quantifies the intensity of absorption by CoO [$0.657 \text{ (mol. \%)}^{-1} \text{ mm}^{-1}$] and it is called as the apparent extinction coefficient. Subsequently, by adjusting the linear region of the Lambert–Beer dependence, it is possible to obtain an equation enabling to calculate the penetration depth (d_p) in an illuminated material for the wavelength used:

$$d_p = \frac{\log(e)}{c \cdot \varepsilon} \quad (3)$$

where c is the CoO content in mol. % and ε corresponds to the apparent extinction coefficient in $(\text{mol. \%})^{-1} \text{ mm}^{-1}$. The penetration depth at a wavelength of 532 nm decreases with the increasing CoO content and reached values in the range between 0.19 (3.55 mol. % of CoO) and 4.40 mm (0.15 mol. % of CoO). Thus, the sample with the suitable penetration depth can be chosen for applications associated with the direct laser writing.

Raman spectroscopy

The structure of glasses prepared by the optimized method was examined by Raman spectroscopy. The spectra obtained were normalized to the maximum of the most intensive band ($\approx 1024 \text{ cm}^{-1}$) of the spectrum of unmodified glass (without CoO). According to the literature [14], in the case of unmodified glass (55PbO-10ZnO-35P₂O₅), the phosphate structural network should consist of a mixture of di-, tri- and tetra-phosphates completed by the PO₃-end structural units. In addition, the Pb-O-P cross linkings are formed and thus, the structure is more connected and compact. In Fig. 5, the comparison of selected Raman spectra is shown, when the spectra for unmodified sample (with 0 mol. % of CoO) and glass with the highest CoO content (3.55 mol. %) were mutually confronted. It seems that the addition of CoO has not affected significantly the structure of the prepared glasses.

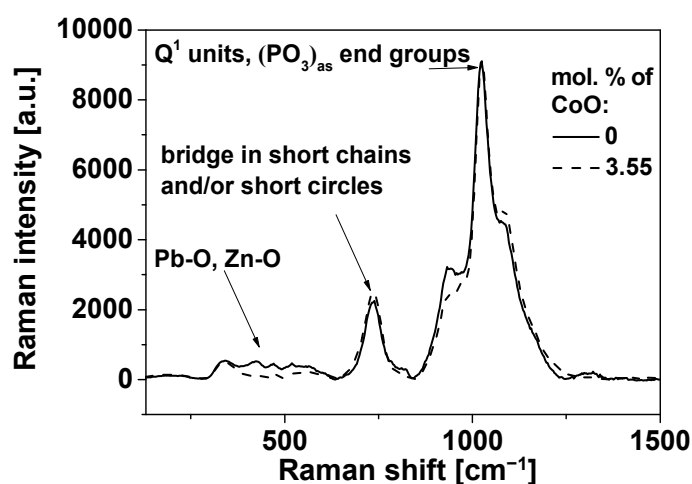


Fig. 5 Reduced Raman spectra of selected glasses (containing 0 and 3.55 mol. % of CoO) normalized to the maximal intensity band in the spectrum for unmodified glass

Electrical properties

Fig. 6 shows the temperature dependence of the DC electrical conductivity (σ) for the two glasses with 0 and 3.55 mol. % of CoO; i.e., for unmodified material and glass with the highest CoO content.

The decrease in the DC electrical conductivity with the addition of CoO can be explained by the formation of “cobalt barriers” which hinder the transport of the carrier in the glass. Since CoO is not a glass-network former, the Co²⁺ ions are isolated in the glass structure, causing the obstruction in the hopping of electrons due to the lack of oxygen bonds. A similar lowering of conductivity was also observed in V₂O₅-CoO-TeO₂ glasses [24].

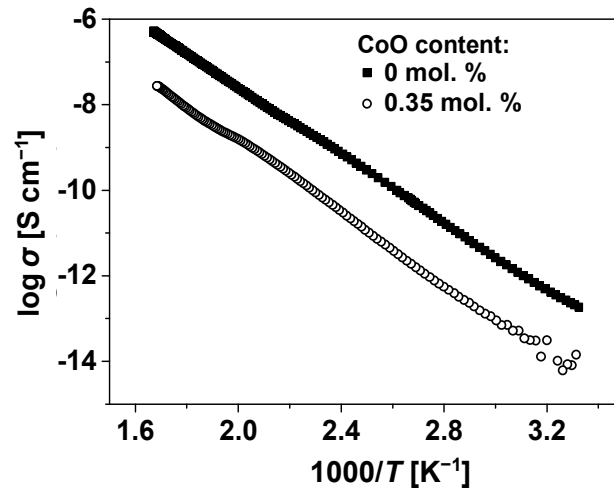


Fig. 6 DC electrical conductivity dependence on the temperature for the selected materials containing 0 and 3.55 mol. % of CoO

The pre-exponential factor σ_0 and activation energy of DC electrical conductivity E_a for the temperature region of 350–435 K was determined from Arrhenius equation:

$$\sigma = \sigma_0 \cdot e^{-\frac{E_a}{K_B T}} \quad (4)$$

where K_B is Boltzmann constant (eV K^{-1}) and T corresponds to the absolute temperature (in K). From Table 2, it is evident that the values of E_a fluctuate in the interval $\Delta E_a (\text{max} - \text{min}) = 0.15 \text{ eV}$ for the samples with the varying CoO content, which is an insignificant change with respect to the experimental error ($\pm 5 \%$).

The conductivity mechanism for the ascertained values of σ_0 can be explained by the transport of carriers excited into the localized states at the band edges and hopping at energies close to the localized state energies near the valence or conduction bands (E_A or E_B) [25].

Table 2 The pre-exponential factor σ_0 and activation energy of electrical conductivity E_a (both based on the Arrhenius equation) obtained for prepared glasses with the various content of CoO (0–3.55 mol. %)

CoO content [mol. %]	σ_0 [S cm ⁻¹]	E_a [eV]
0	0.81	0.75
0.15	0.03	0.81
0.46	0.24	0.78
0.91	9.35	0.90
1.81	0.02	0.80
3.55	1.52	0.88

Conclusions

In this work, 55PbO-10ZnO-35P₂O₅ glasses modified by various amounts of CoO (0–3.55 mol. %) were prepared. The way of synthesis was optimized to obtain glasses with the required quality; i.e., being transparent for the light and thus exhibiting no presence of crystallites, defects, cracks or bubbles. The *wet method* using dilute H₃PO₄ and Co(NO₃)₂·6H₂O powder seems to be the optimal way to meet these requirements. Consequently, the prepared glasses were characterized by several methods in order to obtain the basic characteristics, namely the density, molar volume, thermal and optical properties, structure and electrical properties. The role of CoO content on these properties was discussed. As confirmed, the modification of the glassy matrix by the Co²⁺ ions causes the absorption at 532 nm, which is important for further research that will be focused on the laser direct writing and the formation of microlenses when setting the above-specified wavelength.

Acknowledgements

This research was supported by the Grant Agency of the Czech Republic (No. 19-11814S) and by the University of Pardubice (No. SGS_2019_006). The authors thank Veronika Zemanová, Jan Edlman, Jan Mužátko, and Jan Slavík for their help with measurements.

References

- [1] Yadav A.K., Singh P.: A review of the structures of oxide glasses by Raman spectroscopy. *RSC Advances* **5** (2015) 67583–67609.
- [2] Volf M.B.: *The chemistry of glass* (in Czech). SNTL, Praha 1978.
- [3] Brow R.K.: The structure of simple phosphate glasses. A review. *Journal of Non-Crystalline Solids* **263–264** (2000) 1–28.
- [4] Holubová J., Černošek Z., Černošková E.: Structural investigation and physical properties of Ga₂O₃-ZnO-P₂O₅ glasses. *Journal of Non-Crystalline Solids* **454** (2016) 31–38.
- [5] Day D.E., Wu Z., Ray C.S., Hrma P.: Chemically durable iron phosphate glass wasteforms. *Journal of Non-Crystalline Solids* **241** (1998) 1–12.
- [6] Knowles J.: Phosphate based glasses for biomedical applications. *Journal of Materials Chemistry* **13** (2003) 2395–2401.
- [7] Morena R.: Phosphate glasses as alternatives to Pb-based sealing frits. *Journal of Non-Crystalline Solids* **263–264** (2000) 382–387.
- [8] Campbell J.H., Suratwala T.I.: Nd-doped phosphate glasses for high-energy / high-peak-power lasers. *Journal of Non-Crystalline Solids* **263–264** (2000) 318–341.

- [9] Boetti N., Pugliese D., Ceci-Ginistrelli E., Lousteau J., Janner D., Milanese D.: Highly doped phosphate glass fibers for compact lasers and amplifiers: A Review. *Applied Sciences* **7** (2017) 1295–1312.
- [10] Poirier G., Nalin M., Cescato L., Messaddeq Y., Ribeiro S.: Bulk photochromism in a tungstate-phosphate glass: A new optical memory material? *The Journal of Chemical Physics* **125** (2006) 161101–161104.
- [11] Schwarz J., Tichá H., Tichý L.: Temperature shift of the optical gap in some PbO–ZnO–P₂O₅ glasses. *Materials Letters* **61** (2007) 520–522.
- [12] Salagram M., Krishna Prasad V., Subrahmanyam K.: Optical band gap studies on $x\text{Pb}_3\text{O}_4-(1-x)\text{P}_2\text{O}_5$ lead[(II,IV)] phosphate glasses. *Optical Materials* **18** (2002) 367–372.
- [13] Bach H., Neuroth N.: *The properties of optical glass*. Springer, New York 1998.
- [14] Schwarz J., Tichá H., Tichý L., Mertens R.: Physical properties of PbO–ZnO–P₂O₅ glasses I. Infrared and Raman spectra. *Journal of Optoelectronics and Advanced Materials* **6** (2004) 737–746.
- [15] Tichá H., Schwarz J., Tichý L., Mertens R.: Physical properties of PbO–ZnO–P₂O₅ glasses II. Refractive index and optical properties. *Journal of Opto-electronics and Advanced Materials* **6** (2004) 747–753.
- [16] Liu H.S., Chin T.S., Yung S.W.: FTIR and XPS studies of low-melting PbO–ZnO–P₂O₅ glasses. *Materials Chemistry and Physics* **50** (1997) 1–10.
- [17] Shuker R., Gammon R.W.: Raman-scattering selection-rule breaking and the density of states in amorphous materials. *Physical Review Letters* **25** (1970) 222–225.
- [18] Mayer N.A., Cupid D.M., Adam R., Reif A., Rafaja D., Seifert H.J.: Standard enthalpy of reaction for the reduction of Co₃O₄ to CoO. *Thermochimica Acta* **652** (2017) 109–118.
- [19] Januszka A., Nowosielski R.: Structure and density of Fe₃₆Co₃₆B_{19.2}Si_{4.8}Nb₄ bulk glassy alloy. *Journal of Achievements in Materials and Manufacturing Engineering* **52** (2012) 67–74.
- [20] Lide D.R.: *CRC handbook of chemistry and physics: A ready-reference book of chemical and physical data*. CRC-Press, Boca Raton 1995.
- [21] Holubová J., Černošek Z., Hejda P.: The influence of niobium on the structure of Nb₂O₅–ZnO–P₂O₅ glasses. *Journal of Non-Crystalline Solids* **502** (2018) 35–43.
- [22] Klikorka J., Hájek B., Votinský J.: *General and inorganic chemistry* (in Czech). SNTL, Prague 1989.
- [23] Abdelghany A.M., ElBatal F.H., ElBatal H.A., EzzElDin F.M.: Optical and FTIR structural studies of CoO-doped sodium borate, sodium silicate and sodium phosphate glasses and effects of gamma irradiation. A comparative study. *Journal of Molecular Structure* **1074** (2014) 503–510.
- [24] Sakata H., Sega K., Chaudhuri B.K.: Multiphonon tunneling conduction in vanadium-cobalt-tellurite glasses. *Physical Review B* **60** (1999) 3230–3236.
- [25] Mott N.F., Davis E.A.: *Electronic processes in non-crystalline materials*. Clarendon Press, Oxford 1979.